Remote Sensing of Environment 136 (2013) 374–385

Contents lists available at SciVerse ScienceDirect

Remote Sensing of Environment

journal homepage: www.elsevier.com/locate/rse

Mapping surface temperature in a hyper-saline lake and investigating the effect of temperature distribution on the lake evaporation

S. Sima [a,*], A. Ahmadalipour [a], M. Tajrishy [b,1]

[a] Department of Civil Engineering, Sharif University of Technology, Azadi Ave., Tehran, Iran
[b] Department of Civil Engineering, Sharif University of Technology, P.O. Box 11365-9313, Azadi Ave., Iran

ARTICLE INFO

Article history:
Received 14 February 2012
Received in revised form 5 May 2013
Accepted 20 May 2013
Available online xxxx

Keywords:
Water surface temperature
MODIS
Hyper-saline lakes
Spatial variation
Temporal variation
Urmia Lake

ABSTRACT

Remote sensing is an effective tool for capturing spatial and temporal variations of water surface temperature (WST) in large lakes. The WST of Urmia Lake in northwestern Iran was examined from 2007 to 2010, using MODIS land surface temperature (LST) products. Spatial and temporal (diurnal, monthly, seasonal and inter-annual) variations of Urmia Lake WST were also investigated. Results indicate that the MODIS-derived WSTs are in a good agreement with the in situ data ($R^2 = 0.92$ and bias $= -0.27$). Spatial analysis of WST revealed that there are three thermal zones along the lake: the shallow region in barriers of the causeway, islands and the shoreline; the south part; and the deep north parts. Using validated MODIS-derived WST, the annual temperature cycles of Urmia Lake were extracted and quadratic curves were fitted to empirically display the monthly lake-averaged variations of the lake WST. Then the effect of including the spatial distribution of WST on the lake evaporation was assessed. According to the results of the energy balance method, a 147 mm/year (515 million m^3) discrepancy can be expected in the estimated evaporation rate when the spatial distribution in the lake WST is considered in the energy balance equation. Findings of this study confirm the application of MODIS LST products for surface temperature studies in a large hyper-saline lake. Moreover, use of the distributed satellite-derived WST in estimating evaporation from the lake was shown to improve the accuracy of water loss in the lake water budget calculation.

1. Introduction

Water surface temperature (WST) is a key variable in water quality, and hydrodynamic conditions of lakes (Horne & Glodman, 1994; Lerman et al., 1995). Temperature gradients between the water surface and surrounding atmosphere determine energy and moisture exchange at the air–water interface and thus evaporation losses. Therefore, acquiring WST is a prerequisite to examine the hydrological cycle over lakes and to determine trends in WST attributed to anthropogenic and natural causes (Coll et al., 2005; Reinart & Reinhold, 2008; Schneider & Hook, 2010).

Remote sensing is an effective tool for assessing the temperature cycle of large lakes. It can provide a continuous worldwide record of WST for inland waters and can give insight to global climate changes (Bussières et al., 2002; Novo et al., 2006; Oesch et al., 2008; Schneider & Hook, 2010; Schneider et al., 2009). Retrieving land surface temperature from space is currently possible by various remote sensing platforms e.g., Terra/Aqua-MODIS, Terra-ASTER, NOAA-AVHRR, Meteosat-MVIRI, the ATSR series of instruments and Landsat (Langer et al., 2010; Steissberg et al., 2005). Nevertheless, some of these satellites (e.g., Landsat and ASTER) acquire data with a coarse temporal resolution, which restricts tracing the short-term (e.g., daily or weekly) variations of WST. This low temporal resolution creates high uncertainty for estimates of monthly and annual variations in WST. The moderate resolution imaging spectro-radiometer (MODIS) on board the Terra and Aqua satellites has a large scan angle, which allows for daily data collection (Justice et al., 1998). It has also a high spectral resolution and a moderate spatial resolution varying between 250 m and 1 km (Savtchenko et al., 2004). MODIS is suitable for limnological studies because of the positions of its spectral bands, the instrument's high radiometric resolution, and the relatively easy access of its data (Reinart & Reinhold, 2008).

A number of researches have reported the successful use of MODIS temperature products for studying temperature cycles in water bodies. MODIS SST products were used to map the WST of Lake Geneva and Lake Constance in Europe. Validation results for daytime MODIS SST showed a bias ranging from 0.8–1.9 K and a SD from 0.6–1.1 K, while during nighttime, bias and SD were found to be −0.73–0.45 K and 0.6–1.5 K, respectively (Oesch et al., 2005). An example of recent studies includes monitoring surface temperature of Lakes Vänern and Vättern in Sweden using the MODIS/Terra SST products. A coefficient of determination (R^2) of 0.99, a cool bias of −0.65 °C, an SD value of 0.4 K and a mean absolute error (MAE) of 0.41 K between the daytime satellite data and in situ temperatures were reported (Reinart & Reinhold, 2008). MODIS images were

* Corresponding author. Tel.: +98 21 66164185.
E-mail addresses: sima@mehr.sharif.edu (S. Sima), ahmadalipour.ali@gmail.com (A. Ahmadalipour), tajrishy@sharif.edu (M. Tajrishy).
[1] Tel.: +98 21 6 6164182.

0034-4257/$ – see front matter © 2013 Elsevier Inc. All rights reserved.
http://dx.doi.org/10.1016/j.rse.2013.05.014

also used in conjunction with the AVHRR data to investigate the WST of Lake Malawi. The R^2 and bias were found to be 0.68 and 0.681, respectively (Chavula et al., 2009). In a study conducted on six lakes in California and Nevada, the long-term trends of WST were determined using the nighttime along track scanning radiometer (ATSR) and MODIS data. They used in situ data of Lake Tahoe for validation and obtained a low bias of −0.007 °C and SD of 0.32 °C between the MODIS-LST and in situ data (Schneider et al., 2009). MODIS/Terra LST products were used to extract a time series of daytime and nighttime monthly mean temperatures of Itumbiara hydroelectric reservoir in Brazil. Then, temperature maps were applied to analyze the surface energy budget of the lake (Alcântara et al., 2010). A few studies have applied satellite data to investigate the WST of saline lakes. For example, MODIS imageries were used to examine spatial, diurnal, monthly, seasonal, and annual variations in the water surface temperature of the Great Salt Lake in USA (Crosman & Horel, 2009). The WST of the Dead Sea was mapped using Meteosat Second Generation (MSG) (the European geostationary satellite operated by the European Organization for the Exploitation of Meteorological Satellites) (Nehorai et al., 2009).

Detailed information about the WST of a lake can be used to estimate evaporation as one of the major hydrologic fluxes. Quantifying evaporation from a lake is essential for the lake water budget calculation and for effective lake–basin management (Lenters et al., 2005; Rosenberry et al., 2007). Several methods have been developed to estimate evaporation from water bodies. They can be mainly categorized into the following classes: (1) measurement using evaporation pans and eddy covariance method (2) water balance (3) energy balance (4) mass transfer and (5) combination methods (Gianniou & Antonopoulos, 2007). Amongst all developed methods, the energy budget has been considered as the most robust and accurate technique for determining evaporation (Gunaji, 1968; Harbeck et al., 1958; Sturrock et al., 1992; Winter et al., 2003). It has a 15% error in estimating monthly evaporation rates (Winter, 1981).

The energy balance method has widely been used to evaluate the evaporation from many large lakes including Lake Tahoe, USA (Myrup et al., 1979); Williams Lake, USA (Sturrock et al., 1992); Lake Victoria, USA (Yin & Nicholson, 1998); Lake Flevo, the Netherlands (Keijman, 1974); Lake Vegoritis, Greek (Gianniou & Antonopoulos, 2007); Lake Ziway, Ethiopia (Melesse et al., 2009; Vallet-Coulomb et al., 2001), and Lake Malawi, East Africa (Lyons et al., 2011). However, there are a limited number of studies that use the energy balance method for estimating evaporation from saline lakes (e.g., the Aral Sea (Benduhn & Renard, 2004; Small et al., 1999); the Dead Sea (Lensky et al., 2005; Neumann, 1958)).

For large terminal lakes located in arid and semi-arid regions the water balance highly depends on evaporation. This is particularly true for large shallow lakes like Urmia Lake in Iran, where the negative water balance can lead to the desiccation of vast areas of the lake shores. These salt lands are prone to produce wind-blown “salt-storms”, which can threaten the health and livelihood of the Urmia basin's inhabitants (UNEP & GEAS, 2012). Little is known about Urmia Lake WST as a principal variable in calculating lake evaporation. With the exception of some occasional measurements, there is no continuous time series of the lake WST. Moreover, spatial and temporal variations of WST within the lake are highly unknown. Few studies have investigated evaporation from Urmia Lake. Most of them are based on interpolation of pan evaporation data of synoptic stations surrounding the lake and applying a reduction coefficient to consider the salinity effect (e.g., Sadra Consulting Engineers, 2005; Yekom Consulting Engineers, 2002). The effect of salinity on the pan evaporation was studied by Ahmadzadeh Kokya and Ahmadzadeh Kokya (2008). They compared the two empirical formulas: Meyer (1915) and Harbeck et al. (1958) to calculate the evaporation rate from pans containing water of Urmia Lake. Previous estimates of the evaporation from Urmia Lake using pan evaporation are not accurate enough for water balance calculations due to errors such as the surface effect, salinity influence, instrumental setup and neglecting spatial variation in the lake WST. In this study, we use a modified form of the energy balance method, the Bowen-ratio energy-balance (BREB) method, to provide more accurate estimates of Urmia Lake evaporation.

This study provides the first climatology of the annual WST cycle for Urmia Lake, a large saline lake, and it is also the first study to use spatial estimates of the lake temperature for estimating water loss through evaporation. To accomplish these objectives, MODIS day/night LST data (MOD/MYD11L2, version 5) are used to obtain the surface temperature maps of the lake over the period of 2007–2010. Then, results are validated against in situ measurements. Next, the evolution of Urmia Lake WST in diurnal, monthly, seasonal, and inter-annual time-scales is examined as well as its spatial variation. Furthermore, quadratic curves are fitted to empirically express the monthly variation of the lake WST during the study period. Finally, the effect of incorporating spatial distribution of the lake WST on its evaporation rate is discussed.

2. Study area

Urmia Lake is a shallow terminal lake in the northwest of Iran (37° 04′ N and 38° 17′ N latitude and 45° E and 46° E longitude) (Fig. 1). It is the second largest hyper-saline lake worldwide after the Dead Sea (Zeinoddini et al., 2009). Urmia Lake was declared a wetland of international importance by the Ramsar Convention in 1971 (Ramsar Convention website) and an International Biosphere Reserve by the UNESCO in 1976 (http://www.unesco.org/new/fileadmin/MULTIMEDIA/HQ/SC/pdf/sc_mab_WNBR_BR2012.pdf.). The maximum surface area of the lake has been estimated to be 6100 km^2 but since 1995 it has constantly been declining and was reached 2366 km^2 in August of 2011 (UNEP&GEAS, 2012). There are four major islands in the south part of the lake (Fig. 1) which are important destinations for various migratory birds during winters. A causeway divides the lake into the north and south part with an opening which provides a limited exchange of water between the two sections (Zeinoddini et al., 2009).

The Urmia basin occupies 52,000 km^2 of mainly mountainous terrain. The basin is located at an altitude of 1280 to 3600 m, the lowest part being the lake and its adjacent flat plains. Urmia Lake is surrounded by muddy salt lands, grasslands and croplands mainly developed in the west and southeast of the lake. The climate of the basin is characterized by cold winters and relatively temperate summers. The mean annual rate of precipitation over the lake is about 350 mm, and the mean annual evaporation rate is 900 to 1170 mm. Urmia Lake is supplied by direct precipitation, 21 permanent and ephemeral rivers and 39 intermittent streams mostly discharging into the lake south. Groundwater also supplies a very small fraction of the water inputs to the lake. The long-term average water discharge to the lake was estimated to be about 5300 million m^3 annually. River inflows are highest in spring as a result of snowmelt (Department of Environment, 2010). Because of the progressive dry climate and over-abstraction of water in the lake's drainage basin, water level of the lake has dramatically dropped about 7 m during the past two decades (Hassanzadeh et al., 2012). Simultaneously, salinity has increased to more than 340 g/L. This level of salinity threatens the unique wildlife of the lake, specifically a brine shrimp species, *Artemia urmiana*, which has a high economic value (Karbassi et al., 2010).

Primary factors which control the WST of Urmia Lake include water clarity, salinity, solar forcing, bathymetry, river inflows and wind-induced mixing. The results of hydrodynamic models indicated that wind is the dominant climatic and hydrologic factor determining the lake flow regime, while salinity distribution within the lake is mainly affected by river discharge, evaporation, and rainfall (Zeinoddini et al., 2009). The flow circulation pattern alongside the lake is counter clockwise and the north- to-south and south-to-north flows through the causeway opening are almost equal in most of the year, except in spring when a south-to-north flow dominates as a result of considerable amount of freshwater entering the south lake (Jamali & Marjani, 2007). Moreover, impacts of the wind-induced waves on both water mixing and the salinity distribution/contents of the lake were found to be

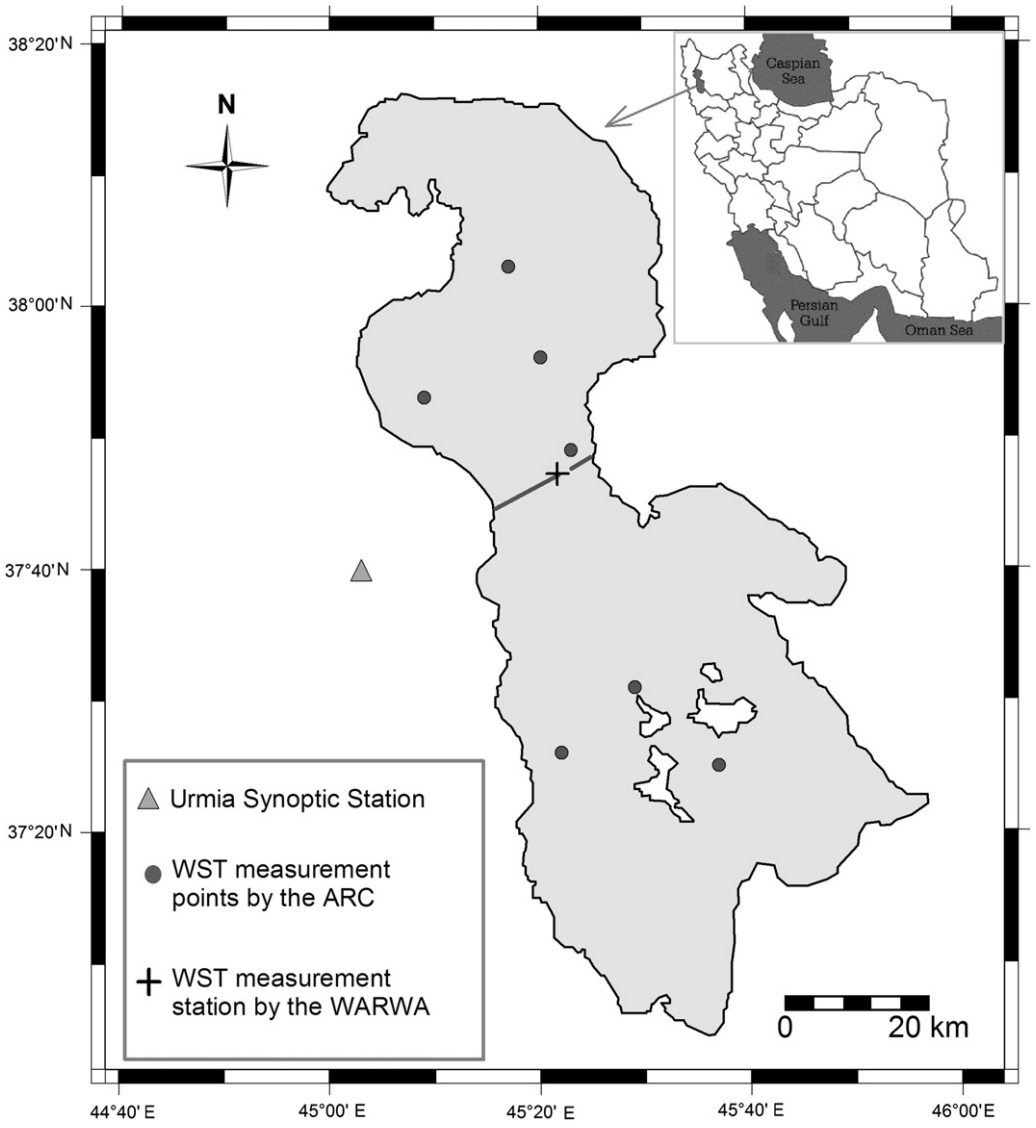

Fig. 1. Urmia Lake in Iran, along with the WST measurement locations.

substantial (Zeinoddini et al., 2013). However, most of these results are based on the models developed for simulating the lake hydrodynamics in the past decades. Since the water inflow and meteorological variables over the lake have been changed significantly, their results are not reliable enough to be applied here.

The high salinity of Urmia Lake inhibits ice formation in winters and controls temperature rise during summer. For saline lakes, the freezing point is lower than 0 °C, and depends on the salt concentration. As the concentration of salt increases, the freezing point drops. For typical oceans water with salinity about 3.5%, the freezing temperature is about −2 °C (UNESCO, 1983). In hyper-saline lakes, having approximately ten times the salt content of ocean waters freezing temperature is much lower. The freezing temperature of Urmia Lake is estimated to be lower than −30 °C. Although sub-zero temperatures have been observed in several parts of the lake during winter months, Urmia Lake water surface has been never frozen.

3. Method

3.1. Satellite data

Several MODIS land and atmosphere products are used in this study to delineate land and water, to control quality, and ultimately to extract surface temperature maps of Urmia Lake (Table 1). These products were acquired from the NASA Active Archive Center (Wan, 2008). MODIS land-surface temperature (LST) level 2, 1-km nominal resolution data (MOD/MYD11L2, version 5) was used to map Urmia Lake WST from 2007 to 2008. MOD/MYD11L2 is produced from MODIS thermal-infrared (11.0–12.0 μm) bands 31and 32 using the split-window algorithm designed for a wide variety of land cover types including inland water surfaces (Wan, 2006).

The region under study is observed during the day between 9 and 12 UTC and at night between 18 and 24 UTC. From the MODIS granules, a region from 36° 30′ to 38° 30′ N and 43° to 46° E containing the study site was extracted. Then using the HDF-EOS to GeoTIFF Conversion Tool (http://www.hdfeos.org/software/heg.php/) the MOD11L2 LST swath files were resampled to a 1 × 1 km grid and UTM projection (Zone 38). For pixels with lower than nominal (1-km) resolution, nearest neighbor interpolation was applied.

Among all available MODIS Terra and Aqua imagery, a total of 393 daytime and 397 nighttime clear-sky images were processed for the period of 2007 to 2010. Monthly variation of the available clear-sky images between 2007 and 2010 at day and night are illustrated in Fig. 2a and b, respectively. From December to March, the pronounced cloud cover restricts the availability of clear-sky images, so that in

Table 1
MODIS products used in this study.

Satellite data	Spatial resolution (m)	Temporal resolution	Application
MOD/MYD11L2	1000	Daily	Water surface temperature
MOD/MYD35	1000	Daily	Cloud mask
MCD12Q1	500	Yearly	Water mask
MOD13Q1	250	16 days	Water mask

some years there was no cloud-free image. This limitation prohibited us from providing monthly and seasonal analysis of Urmia lake WST during these months. Moreover, the number of cloud-free imageries increases from spring to summer months. Afterward, from September on a declining trend in the number of cloud-free satellite images is evident. The limited number of cloud-free imageries in early spring and mid-fall causes less confidence in the calculated statistics and retrieved WST variation during these months.

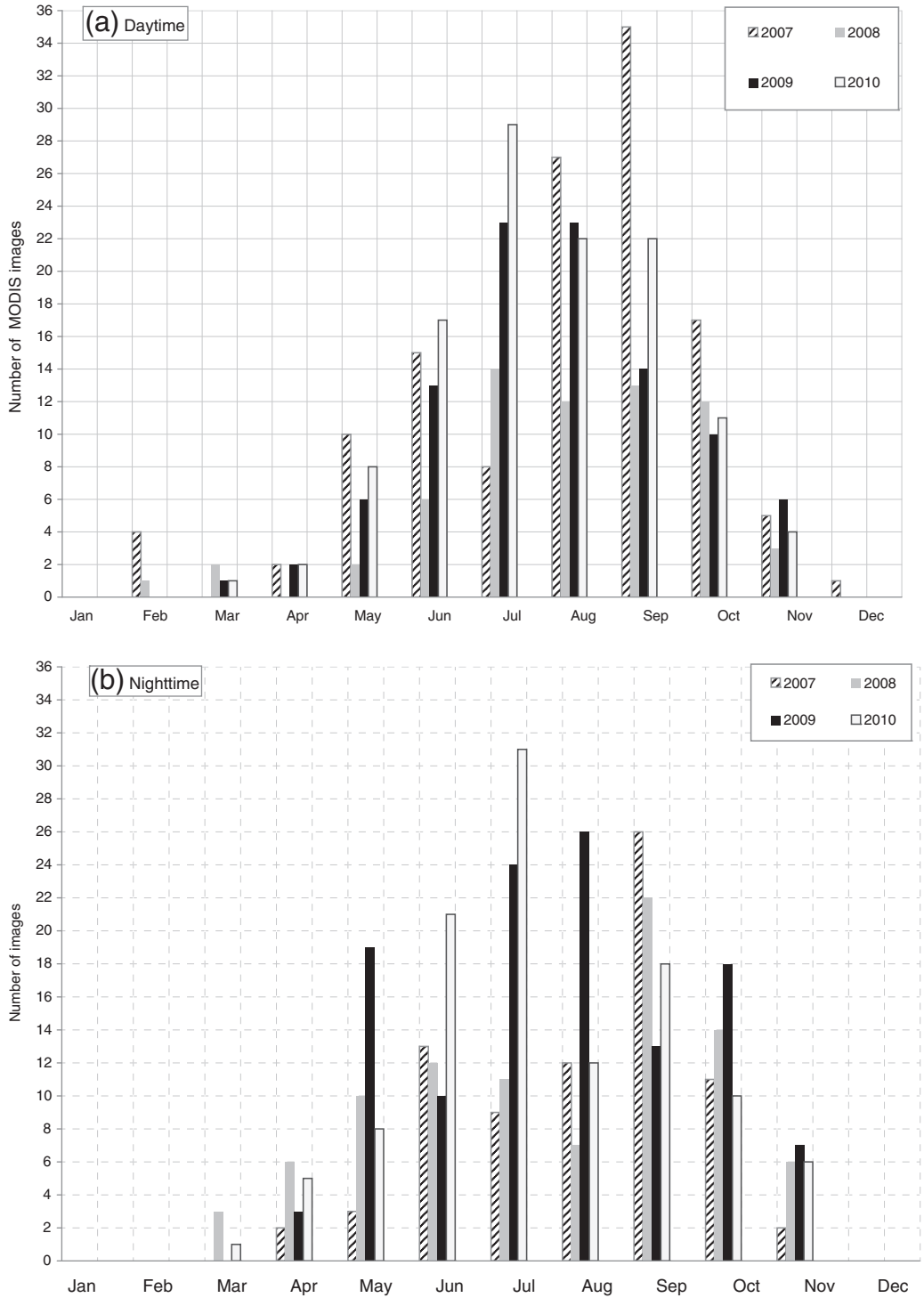

Fig. 2. Number of available cloud-free MODIS-LST images for Urmia Lake between 2007 and 2010: (a) daytime and (b) nighttime.

3.2. Preprocessing of satellite data

3.2.1. Land–water mask

When extracting water surface temperature of a lake, it is crucial to accurately discriminate between land and water areas in advance. Without applying a reliable water mask it is likely to have land contamination in examining the lake WST at land–water interfaces such as shorelines and the islands. In this study, two methods were applied to map Urmia Lake. The first one was using the MODIS land cover products of the study area, while the latter was delineating the lake extents based on the Normalized Difference Vegetation Index (NDVI) thresholds. MODIS yearly land cover products (MCD12Q1) with a spatial resolution of 500 m were applied, and the lake area was identified by zero code in classification schemes of 1 through 4 and class 3 in schemes 5. Since the lake is shallow, the within year variation of the lake areal extent is considerable (Sima et al., 2012). Therefore, other techniques should be applied in conjunction with the land cover maps to capture intra-annual variations of the lake area. As a complementary method, MODIS 250 m NDVI products (MOD13Q1) were acquired to map seasonal variations in the lake area more precisely. Determining threshold values on the NDVI map is amongst commonly applied MODIS-based water classifications (Gao et al., 2012). Water bodies can be recognized by negative values on NDVI maps, which are presented as undefined values on MOD13Q1. Islands can also be distinguished by positive NDVI values. Finally, the seasonally delineated areas of Urmia Lake were applied to extract the lake WST and to separate some anomalously cold or warm pixels at the shoreline of the lake.

3.2.2. Cloud mask and quality control

To avoid cloud contamination, the MOD35 cloud mask product was applied. Images with lower than 20% cloud coverage over the study area were recognized as cloud-free and were used for further processing. MODIS-LST products were also checked for other quality issues by using quality assurance flags. The satellite zenith angles of LST products were restricted to less than 55° in order to prevent the non-Lambertian effects on emissivity at high view angles. Excluding poor quality data, 805 MODIS-LST (Terra/Aqua) images were available for the lake WST analysis in the period of 2007–2010.

3.3. In situ data of Urmia Lake WST

Conventionally, temperature monitoring in large lakes is carried out using permanently-deployed buoys. In Urmia Lake, however, there is no such equipment, so most of the temperature measurements have been conducted from the lake shores and temperature data from the interior parts of the lake are sparse. For example, the lake bulk temperature was measured by the West Azarbaijan Regional Water Authority (WARWA) in a fix point near the causeway (see Fig. 1), from October 2009 to September 2010 twice a day at 12:00 and 14:00 local time. Such measurements are not appropriate for validation of the satellite-derived WST because of the possibility of land contamination. Instead, temperature measurements from the deep waters, far from the lake shores, are required.

Amongst several institutes studying Urmia Lake, the Artemia Research Center (ARC) has collected water quality samples from six deep points within the lake and have measured WST from 2001 to 2006 (see Fig. 1). Although our study did not cover this time period, we used the WST data of the ARC and their concurrent MODIS-LST products for the purpose of validation. This is due to the lack of temperature data from the interior parts of the lake. Moreover, during our survey to monitor water quality of the lake between 2009 and 2010, the lake surface temperature was measured in several samples collected from the interior parts of the lake. Overall, considering the cloud-free satellite images in the period of the two water quality studies and the in situ measurements taken within 1 h of the satellite retrieval, a total of 46 match-ups were obtained and were used for the validation. Since all temperature measurements have been performed between 10:15 to 15:15 local time, just the daytime WST images were used for validation.

3.4. Considering spatial distribution of WST in estimating Urmia Lake evaporation

To assess the effect of including spatial distribution of Urmia Lake WST on evaporation estimates, monthly maximum evaporation rates during 2009 were calculated using the BREB method. Typically, the WST of Urmia Lake is measured at several locations on the lake (mostly shorelines) and the data is used as the WST of the whole lake. Nevertheless, shoreline measurements are not appropriate indicators of the lake surface temperature since they are overestimations of the lake WST.

To evaluate the importance of considering the spatial distribution of the lake WST on evaporation estimates, the energy balance equation was run twice. In the first run, the monthly lake-averaged MODIS-derived daytime WSTs were used as the mean monthly WSTs of the lake. In the second run, the monthly in situ temperature data at the WARWA measurement station were assumed to be representative of the lake monthly WSTs (see Fig. 1). Then the results were compared in terms of monthly and annual evaporation rates. It should be noted that since in situ temperature data were only available for daytime, nighttime images were not used for the comparison. Therefore, the calculated evaporation rates are not the mean monthly rates. Instead, they are approximations of the maximum monthly evaporation rates. This is due to the fact that the daytime satellite passes are roughly concurrent with the time of maximum daily solar radiation and thus corresponding evaporation rates are close to maximum daily rates of evaporation.

3.4.1. BREB method

The BREB method (Winter et al., 2003) for calculating open-water evaporation is formulated as:

$$E = \frac{Q_{SN} - Q_{LW} - Q_n + Q_{AD} - Q_b}{\rho L_e (1 + B)} \quad (1)$$

where

E	evaporation rate (m s^{-1})
Q_{SN}	net short-wave radiation (W m^{-2})
Q_{LW}	net long-wave radiation (W m^{-2})
Qn	net heat flux which is the change in heat stored in the lake-water body (W m^{-2})
Q_{AD}	net advected heat into the water body from precipitation, surface water, and ground water (W m^{-2})
Q_b	net energy conducted from the lake to the sediments (W m^{-2})
ρ	density of brine (kg m^{-3})
L_e	latent heat of vaporization (J kg^{-1})
B	Bowen ratio (dimensionless).

Q_{AD}, Q_n and Q_b often are very small and are commonly ignored (Rosenberry et al., 2007). Net short-wave radiation can be calculated from the following equation:

$$Q_{SN} = (1 - \alpha) Q_{Sin} \quad (2)$$

where α is the water surface albedo, and Q_{sin} is the incoming solar radiation which can be computed from Savinov–Angestrom formula (Budyko, 1974):

$$Q_{Sin} = \left(\alpha + b\frac{n}{N}\right) Q_0 \quad (3)$$

where a, b are the local regression parameters and n, N are the actual and maximum possible hours of sunshine, respectively.

Net long-wave radiation is the difference between the upward infrared radiation emitted by the water body and the atmospheric radiation reaching its surface. It is obtained from the Clark et al. (1974) formula:

$$Q_{LW} = k_b \varepsilon \cdot T_s^4 (0.39 - 0.05\sqrt{e_a})\left(1 - 0.69C^2\right) + 4k_b \varepsilon \cdot T_s^3 (T_s - T_a). \quad (4)$$

T_s and T_a are the lake surface and air temperature in K, k_b is the Boltzmann coefficient, ε is the emissivity of the water body, C is the cloud cover and e_a is the atmospheric vapor pressure measured at Urmia synoptic station. Eq. (4) indicates the important role of the lake WST in calculating net long-wave radiation and thus the resultant evaporation estimate.

The Bowen ratio is the ratio of sensible to latent heat and is calculated as:

$$B = c_b \frac{T_s - T_a}{e_{brine} - e_a} \cdot \frac{P}{1000} \quad (5)$$

where P is the atmospheric pressure (mbar) and c_b is the Bowen's constant, typically 0.61 1/°C (Bowen, 1926; Rubin & Atkinson, 2001). The vapor pressure of Urmia brine, e_{brine}, is lower than that of freshwater, by a factor a_{H_2O}, which is the water activity (Salhotra et al., 1985):

$$e_{brine} = a_{H_2O} \cdot e_{sat}(T_s) \quad (6)$$

The saturation vapor pressure in turn, is computed using the Magnus–Tetens formula:

$$e_{sat}(T_s) = 0.6105 \exp\left(\frac{17.2T_s}{T_s + 237.3}\right) \quad (7)$$

where T_s is the water surface temperature in °C and e_{sat} in mbar.

3.4.2. Model input parameters

Model inputs can be classified in three groups: meteorological variables over the lake, Urmia Lake physico-chemical parameters, and constants. For meteorological variables such as T_a, P, e_a and n, it was assumed that weather condition at Urmia synoptic station (depicted by a triangle in Fig. 1) resembles the climate over the entire lake. Since there is no weather station installed on the lake, distribution of the climatic variables over the lake is completely unknown. Hence, the meteorological data measured at the nearest synoptic station to the lake (Urmia Station) were used. Values of Urmia Lake physico-chemical parameters and constants were obtained from field surveys and literature (Table 2).

Table 2
Urmia Lake physico-chemical parameters, and constants used as an input data in the BREB model.

Data	Description	Value	Units	Reference
Lake parameters	Density (ρ_{brine})	1203	kg/m^3	Heidari et al. (2010)
	Activity of Urmia brine	0.77	–	Heidari et al. (2010)
	Emissivity (ε)	0.98	–	Masuda et al. (1988), Niclòs et al.(2005)
	Albedo (α)	0.07	–	Lenters et al. (2005)
Constants	a,b	0.32, 0.5		Jamab Consulting Engineering (1998)
	Boltzmann coefficient (K_b)	5.67×10^{-8}	W/m^2 K^4	Clark et al. (1974)
	Bowen's constant	0.61	mbar/°C	Bowen (1926)

4. Results and discussions

4.1. Validation

To assure the accuracy of satellite data, it is essential to validate the satellite-derived surface temperature against in situ measurements. Validations of the satellite-derived surface temperature have mostly been conducted for oceanic waters (e.g., McAtee et al., 2007; Meguro et al., 2004; Sumner et al., 2003); however, several attempts have been made to validate lake temperatures (e.g., Oesch et al., 2005; Reinart & Reinhold, 2008; Schneider et al., 2009; Thiemann & Schiller, 2003).

For Urmia Lake, the scatter plot of the MODIS-derived WST versus in situ measurements is shown in Fig. 3. It exhibits a cool bias of −0.27 °C as well as a root mean square error (RMSE) of 2.26 °C between the satellite-derived WST and in situ observations. The mean bias error (MBE) and the mean absolute error (MAE) of 0.77 °C and 2 °C are also distinguished between the satellite and in situ surface temperatures, respectively. The standard deviation of in situ WST data is 7.5 °C, whereas for the MODIS-derived WST it is 7 °C, which are close to each other. Moreover, unit slope of the regression line and a $R^2 = 0.92$ indicate that in situ and remotely sensed temperatures are well correlated.

According to Wan (1999), MODIS LST products can be used as valid data if the error analysis indicates that the absolute accuracy of satellite measurements is better than 1 K standard deviation. However, such accuracy was not achieved in this study (SD = 2.4 °C). Although the trend of the satellite-derived WST is well consistent with the trend of in situ bulk temperatures, the error in predicting the absolute values of the lake WST is relatively high. Apart from the potential errors in the satellite-derived WST data including instrument noise and drift, sun glint (Martin, 2005), residual cloud contamination, misspecification of atmospheric attenuation (Harris & Mason, 1992; Robinson et al., 1984) and surface emissivity effects (Liu et al., 1987), the high RMSE and MAE values may arise from the in situ WST data which were not collected for the aim of WST validation and may suffer from instrumental errors.

The small cool bias of 0.27 °C can be mainly resulted from the cool skin effect, and influence of the warm layer is negligible since the lake is shallow and thermally is non-stratified. The cool skin and the warm layer effects can result in 0.1 to 0.6 and 0.5 to 5.0 °C temperature deference, respectively (Harrocks et al., 2003). The calculated cool bias of Urmia Lake WST falls within the reported range in the literature. The relationship between skin and bulk temperatures, however, is complicated and depends upon several parameters such as dominant wind speeds, the time of the day, and the depth of the measurements (Donlon et al., 2002; Hook et al., 2003, 2007). The largely unknown spatial and temporal variations in wind speed and net heat flux through

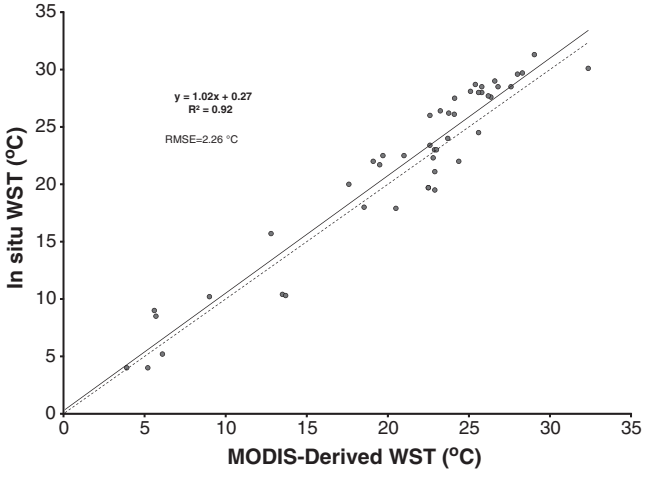

Fig. 3. Comparison of the MODIS-derived WST with in situ bulk temperature.

Urmia Lake prohibit the inclusion of the skin effect in this study. Except for the skin effect, in hyper-saline lakes salinity and turbidity of water have a minor influence on the emissivity variations, which leads to a slight cool bias in the resultant WST (Crosman & Horel, 2009; Wu & Smith, 1997).

4.2. Monthly variation of Urmia Lake WST

Mean monthly maps of the MODIS-derived WST between 2007 and 2010 are presented in Fig. 4 as well as the lake-averaged descriptive statistics (mean, minimum, and maximum). Production of monthly temperature maps was prohibited between December and March because of inadequate cloud-free images.

In general, three distinct thermal zones can be recognized along the entire lake: the shoreline, the islands and the causeway borders (with a depth lower than 1 m) which are so called thermal strips; interior north part; and the south part of the lake. For daytime temperatures, a decreasing pattern from the shoreline toward the lake center is evident, while at night this thermal pattern is inverted. Comparing the WST of the southern parts to the lake north, the southern section is warmer during spring and summer and cooler in fall.

The maximum daytime temperature gradient within the lake occurs in summer months, whereas the spatial difference in the lake WST is minimized in October and November. For nighttime images, the thermal gradient within the lake peaks in fall months. Furthermore, the extent of spatial variation in daytime WST ranges from 3.8 °C in November to 6.7 °C in August. At nighttime, the range of spatial variation in the lake

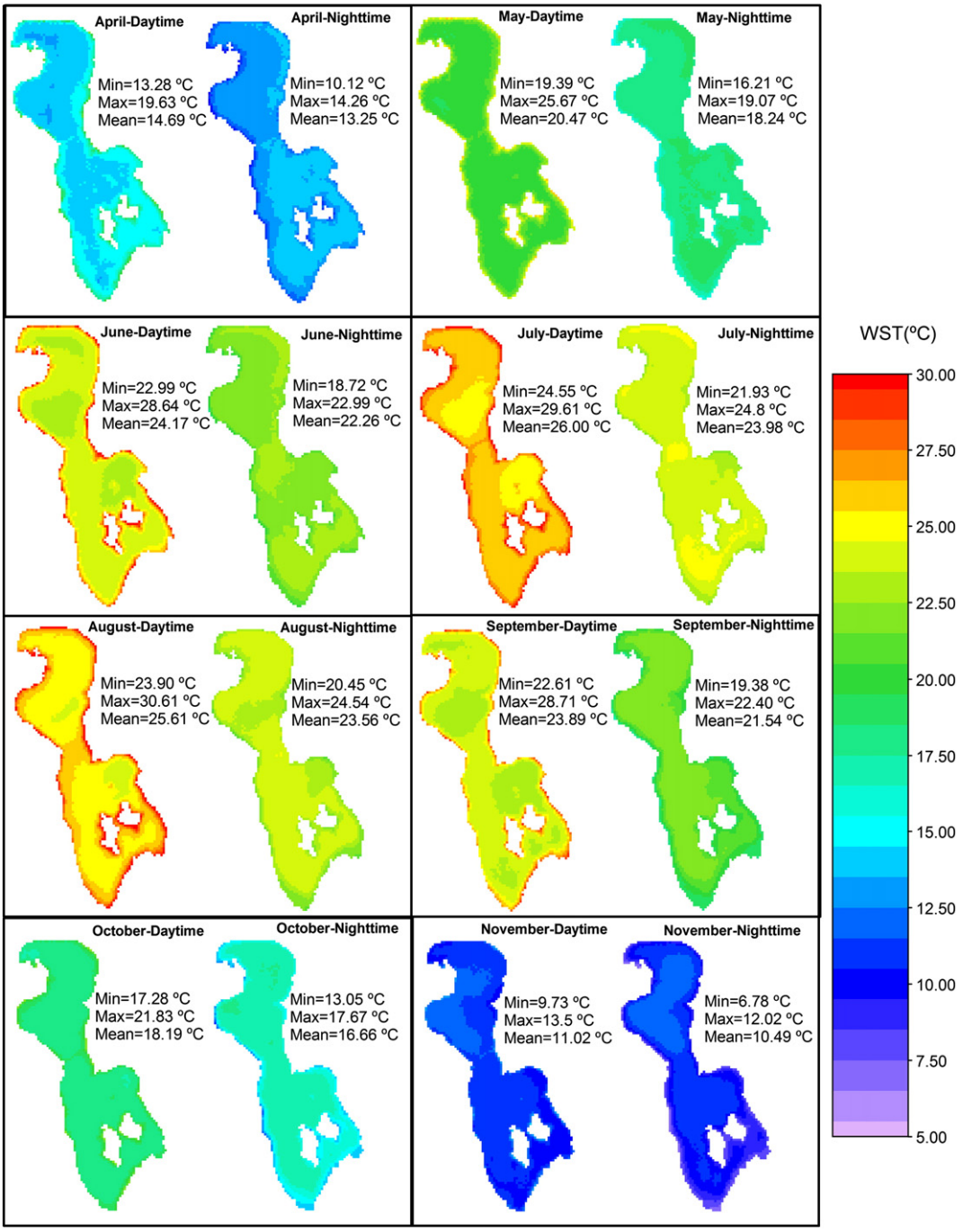

Fig. 4. Mean monthly maps of satellite-derived daytime and nighttime WST for Urmia Lake from 2007 to 2010.

WST ranges from 2.8 °C in May and July up to 5.4 °C in November. In other words, the lake WST is more homogeneous at night compared to the daytime. The high spatial variability in summer also reflects the strong seasonal warming in the thermal strips relative to weaker heating in the deep parts of the lake.

When studying the temperature cycle of lakes, the beginning of ice cover breakup and the time of minimum and maximum water surface temperature are of paramount importance (Bussières et al., 2002). The first two are key parameters for biological and chemical process inside lakes as well as navigation (Adams & Prowse, 1981), while the latter is the peak time of evaporation, which is a determining factor in the hydro-meteorology of lakes. Using the mean monthly MODIS-derived temperature maps, these parameters were examined for Urmia Lake. Because of the high salinity of Urmia Lake, it never ices over. The minimum WST of the lake occurs in November, whereas the maximum values are observed in July for both daytime and nighttime. The mean monthly lake-averaged values of Urmia Lake WST also vary from 11 °C to 26 °C during the day and 10.5 °C to 24 °C at night.

The daytime images indicate that in spring, warming starts from the shallow littoral regions and expands to the interior of the lake (mainly from the southeast). The temperature distribution inside the lake is almost uniform, although the warm strips remain distinct. In summer, the warm up pattern continues. The interior parts at the north and south stay cooler for a long period, since more heat flux is required to increase the temperature of deep regions. During summer months, two warm patches can be distinguished in the north and south parts of the lake. The first one is formed in the north of the causeway, while the latter is in the north east of the islands. These warm patches disappear by fall. In October, cooling starts from shallow thermal strips and spreads toward the interior parts of the lake. The north part of the lake remains slightly warmer compared to the southern part, as a result of a delay in cooling.

The nighttime warming pattern in April is similar to the daytime warming pattern. In May WST distribution along the lake is almost homogeneous. However, in June and July warm patches are formed in the southwestern part of the lake and south of the causeway. In August these patches gradually expand toward the north of the lake. In late summer, the lake WST is almost evenly distributed between the north and south parts. In October, cooling starts from the thermal strips and covers the central deep parts by November.

The delay in warming and cooling of the deep parts of the lake arises from the high thermal mass of the lake central parts compared to the shallow littoral zone (Wells & Sherman, 2001). Since the lake is shallow and its heat storage capacity is low, a fast warming (5.8 °C/month) from April to May, and a fast cooling between September and October (−5.7 °C/month) is expected to be observed in the satellite data. The rate of lake warming in the mid-spring and its cooling in the late summer at nighttime was 5 and −4.9 °C/month, respectively.

Fig. 5 shows the monthly variation of the mean monthly lake-averaged WST difference between the daytime and nighttime. Diurnal variations of Urmia Lake WST increase from April to September and then decrease to about 0.5 °C in November. This can be inferred by the loss of daytime heat flux inputting to the lake surface from the late summer to the end of year. As depicted in Fig. 5, the diurnal temperature difference in Urmia Lake can be up to 2.4 °C.

4.3. Seasonal variation of Urmia Lake WST

Seasonal maps of Urmia Lake WST in the period of 2007 to 2010 are shown in Fig. 6. To determine the seasonal thermal amplitude, the seasonal maps of nighttime were subtracted from daytime maps. The mean daytime WST of Urmia Lake varies seasonally from 25.5 °C in summer to 14.5 °C in fall. At night, the mean seasonal WST decreases from its maximal value of 23 °C in summer to 13.5 °C in fall. Additionally, a positive temperature gradient between the shorelines and the center of the lake can be observed in all seasons.

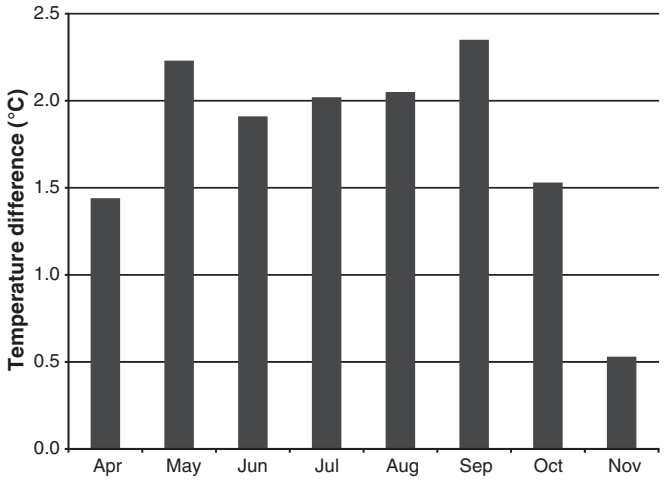

Fig. 5. Monthly variation of WST difference between daytime and nighttime in Urmia Lake from 2007 to 2010.

The mean spatial variation in the daytime WST of the lake is up to 5 °C in summer and less than 4 °C in fall. For nighttime the spatial variation of the lake seasonal WST varies between 2.6 °C in spring to 5 °C in fall. This can be attributed to the reduction in the intensity of solar radiation from summer through winter and an increase in the incoming solar energy in spring. In recent years, the restriction of freshwater inflows to the lake and the reduced seasonal fluctuations of inflows have induced limited circulation inside the lake. This in turn may affect distribution of the lake WST. However, a comprehensive analysis cannot be presented without thorough modeling of the lake hydrodynamic.

During all seasons, the day–night temperature difference is higher at the thermal strips compared to the interior parts because of the buffered temperature change in the central parts of the lake. In the summer, the temperature difference between day and night ranges from 1.5 °C in central deep parts to more than 8 °C in thermal strips. In addition, mean values of the seasonal day–night difference slightly increase between spring and summer and then decrease to 1 °C in fall.

4.4. Inter-annual variation of Urmia Lake WST

The annual cycles of Urmia Lake WST were determined using the MODIS-derived mean monthly maps (Fig. 7). Comparing the annual cycle of the lake daytime WST with the four-year mean, a positive shift in the annual WST cycles is observed in 2007 and 2010, and a negative shift is detected for 2008 and 2009. Moreover, the highest discrepancies from the four-year mean annual cycle occurred in 2010 and 2009 at day and night, respectively.

Inter-annual variability of the seasonal daytime and nighttime MODIS-derived WST is illustrated in Fig. 8. From 2007 to 2010, the daytime WST is nearly constant between 2007 and 2009 and then increases in 2010. In fall, the daytime WST decreases from 2007 to 2008, and after a slight rise up in 2009, it decreases again in 2010. For nighttime, during summer the lake WST steadily decreases until 2009, and then increases in 2010. In spring, following a decrease in the lake WST between 2007 and 2008, WST drops in 2009 and then rises in 2010. In fall, the lake WST decreases between 2007 and 2008 and then remains almost constant until 2010. Overall, amongst the four years of the study, the daytime WST of Urmia Lake was the highest in the summer and spring of 2010 and the lowest in the fall of 2010. At night, the lake WST was lowest in 2009 during all seasons.

4.5. Empirical model to describe annual cycle of Urmia Lake WST

To express the annual cycle of Urmia Lake WST analytically, various curves were fitted to the MODIS-derived lake-averaged mean

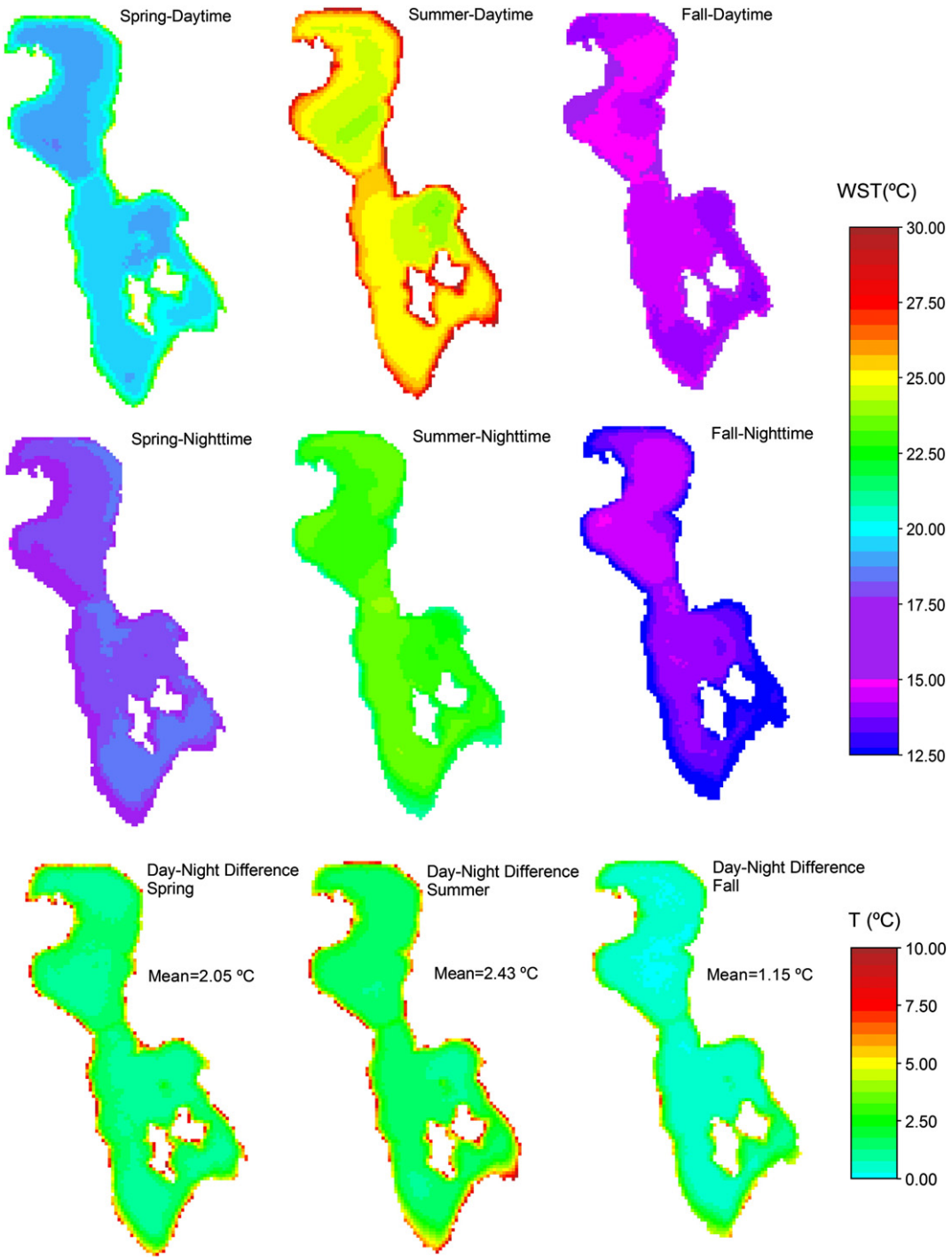

Fig. 6. Seasonal variation of Urmia Lake WST from 2007 to 2010.

monthly temperature values. Quadratic curves were the best fits which properly described the monthly variation of Urmia Lake WST at both daytime and nighttime through 2007 to 2010. Several researchers also confirmed the suitability of quadratic curves to model the annual variations of lakes WST (Bussières et al., 2002; Reinart & Reinhold, 2008). The mean monthly WSTs of Urmia Lake can be formulated as follows:

$$T_s = at^2 + bt + c \quad (8)$$

where, T_s is the water surface temperature in °C, t is the time (in Julian days) of the year under study, and a, b, and c are empirical coefficients determined by the least square fit. For each of the four study years, fitting coefficients are calculated as presented in Table 3. Generally, the coefficient values are close to each other at both daytime and nighttime.

High values of R^2 (0.97–0.99) indicate that quadratic curves can satisfactorily resemble the variation of the lake monthly WST between April and November. Moreover, RMSE, MBE and MAE were calculated to compare the monthly lake-averaged satellite-derived values of WST to the predictions of polynomial fits. According to these performance measures, the lake monthly WSTs were reasonably predicted with maximum RMSEs of 2.6 °C and 1.8 °C, maximum MAEs of 2 °C and 1.5 °C for daytime and nighttime, respectively. Consequently, quadratic curves can

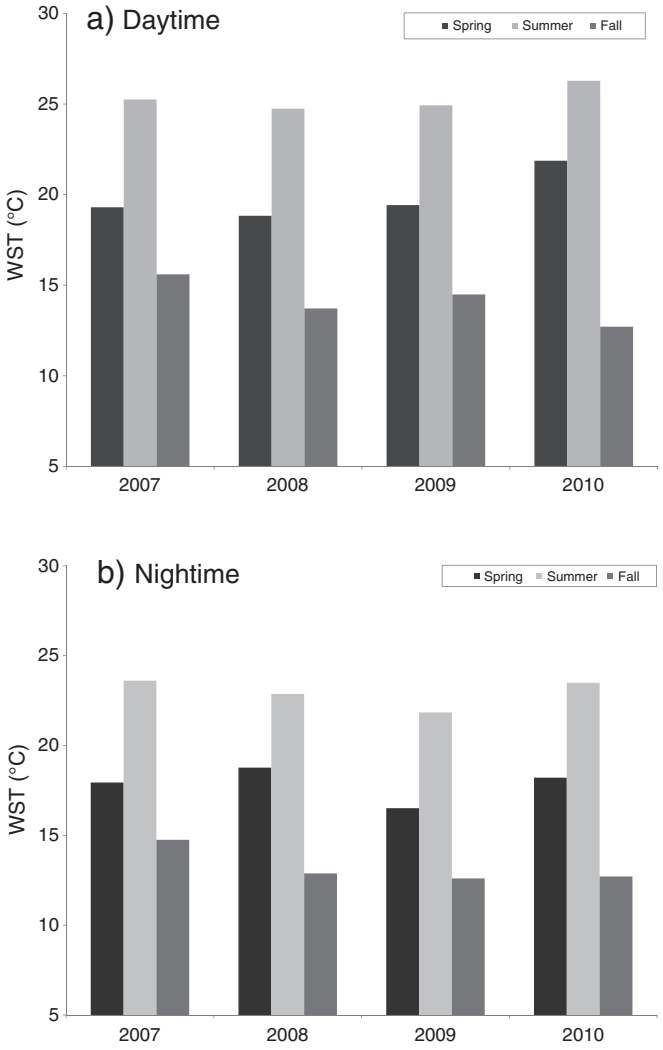

Fig. 7. Annual cycle of the MODIS-derived WST in Urmia Lake from 2007 to 2010.

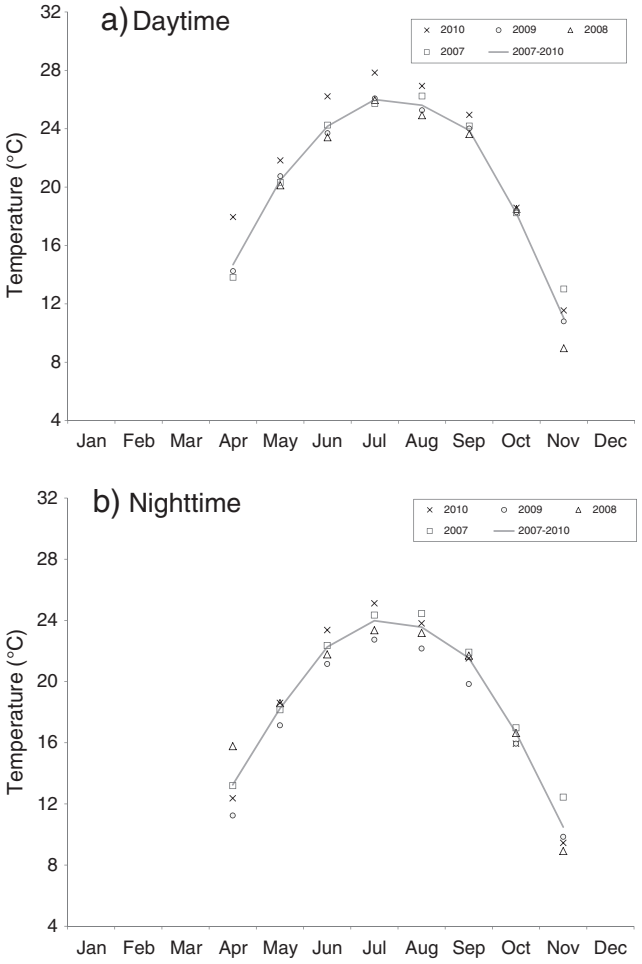

Fig. 8. Inter-annual variation of mean seasonal WST in Urmia Lake from 2007 to 2010.

properly estimate both the trend and values of the mean lake-averaged monthly WST of Urmia Lake in each year.

4.6. Comparison of the lake evaporation rates

The results of the calculated evaporation rates using the MODIS-derived lake-averaged WSTs and WARWA measurement of WST at a single point are tabulated in Table 4. Due to absence of cloud-free satellite images between December and March, the comparison was performed from April to November. Mean annual rate of evaporation was also calculated, by neglecting the lake evaporation during the cold months.

From Table 4, it can be found that the lake evaporation is under-estimated when point WST data are used instead of the satellite-derived lake-averaged WSTs. This is because of the fact that the shoreline measurements of WST are higher than the satellite-derived WSTs, which are obtained based on the temperature distribution within the entire lake. As a result, the corresponding net longwave radiation is higher and the net radiation flux is lower. This in turn leads to a lower evaporation rate, since the net radiation is the dominant term in the energy balance of most lakes.

The monthly difference in the lake evaporation rates constantly increases from April to its peak in July, then decreases from August on. The difference in warm seasons can be as much as 31.5 mm. Moreover, a 147 mm discrepancy can be expected in the lake mean annual evaporation rates where the spatial distribution of the WST is involved in the energy balance equation. Taking into account the vast area of Urmia Lake, this difference can lead to a 515 million m^3 variation in calculating water loss from the lake. This is a substantial amount of water, particularly in semi-arid regions facing water shortage problem. This volume equals to about 30% of the water which has been regulated in the Urmia basin through the construction of 29 dams. Furthermore, the 14% under-estimation of the lake evaporation rate results in over-estimation of the lake water content. Hence, the amount of water allocated to Urmia Lake based on such a water budget would be inadequate. Thus, accurate estimation of evaporation rate from the lake through considering distribution of WST along the lake has a

Table 3
Coefficients of the quadratic curves fitted to empirically display the mean monthly surface temperature of Urmia Lake and corresponding performance measures from 2007 to 2010.

Satellite pass	year	R^2	Coefficient			Performance measures		
			a[°C d^{-2}]	b[°C d^{-1}]	c[°C]	RMSE	MBE	MAE
Daytime	2007	0.991	−0.0012	0.53	−32.13	1.23	−1.00	1.00
	2008	0.983	−0.0014	0.60	−39.78	1.35	−1.97	1.97
	2009	0.992	−0.0012	0.54	−32.68	2.59	0.37	1.51
	2010	0.988	−0.0012	0.51	−26.93	0.71	1.49	0.58
Nighttime	2007	0.990	−0.0011	0.48	−28.90	1.77	−1.49	1.49
	2008	0.967	−0.0010	0.44	−23.13	1.82	1.41	1.59
	2009	0.998	−0.0011	0.49	−31.31	0.86	−0.72	0.73
	2010	0.996	−0.0013	0.56	−35.90	0.27	0.17	0.22

Table 4
Monthly evaporation rate of Urmia Lake (mm/month) calculated using spatial and point MODIS-derived surface temperatures in 2009.

	Apr	May	Jun	Jul	Aug	Sep	Oct	Nov	Annual (mm)
MODIS-derived lake-averaged WST	92.0	157.1	160.0	214.1	185.2	106.6	81.8	35.8	1033
WST measurement at a single point	83.0	142.3	137.2	182.6	156.0	94.9	70.7	18.7	885
Difference	9.0	14.8	22.8	31.5	29.2	11.7	11.1	17.1	147

profound effect on the Urmia Basin water resources management and the lake ecosystem management as well.

5. Summary and conclusions

Because of the sparse continuous measurements of the surface temperature in Urmia Lake, using satellite data is the most appropriate way to detect both temporal and spatial variations. WST of the lake was retrieved during 2007–2010, and its spatial and temporal variations were investigated employing MODIS L2 LST products. Using satellite-derived WSTs, the effect of considering the spatial distribution of WST in the estimation of evaporation rate from the lake was assessed. The main conclusions are as follows:

- The capability of MODIS satellite data is limited by the number of available clear-sky images. For Urmia Lake, in late fall and winter few clear-sky images were available during the study period.
- Urmia Lake WST extracted from the MODIS-LST data reasonably correlate with in situ bulk temperature measurements in Urmia Lake.
- Three thermal zones were distinguished along the lake: the shallow region in barriers of the causeway and islands and the shoreline (thermal strips); the south part; and the deep north parts. Due to the higher heat storage capacity, a delay was observed in the warming and cooling of the deep northern part compared to the southern part of the lake.
- Excluding the cloudy months of December to March, Urmia lake WST is the lowest in November, whereas the maximum values were observed in July for both daytime and nighttime.
- During daytime, temperature gradient within the lake peaks in summer months, whereas the spatial difference in the lake WST minimizes in October and November. For nighttime images, maximum thermal gradient within the lake occurred in fall.
- Monthly variation of Urmia Lake WST from April to November can be well described by a quadratic function at both day and night.
- Taking into account the spatial distribution of Urmia Lake WST in estimating its evaporation leads to a 515 million m^3/year difference in the lake water budget.

In this study, just the effect of including the distribution of WST in estimating evaporation from Urmia Lake was assessed. Application of the distributed meteorological data over the lake can affect estimation of the evaporation rate. This can be addressed either by conducting direct measurements of the climate variables over the lake or through using the spatial interpolation techniques. Supplementary studies should be conducted to investigate the use of spatially distributed meteorological variables over the lake in its evaporation estimation.

One of the shortcomings of this study is the exclusion of the hydrodynamic condition of Urmia Lake in the analysis of the lake WST. Further research is needed to examine the current hydrodynamic condition of the lake (by considering the limited water inflows to the lake and recent variations in the meteorological variables over the lake) and to investigate the interactions between the lake WST and the flow circulation as well as the density distribution alongside the lake.

To improve the confidence in the application of the satellite-derived WSTs, it is required to collect sufficient in situ data from several parts of the lake having various depths. One obstacle for extending the study period is the lack of in situ data for validation of the satellite-derived WST. If continuous measurements of the lake skin temperature are taken using radiometers, satellite-derived WST can be applied more confidently for a long-term period and can be used to provide an insight into the climate change over the lake and its consequences on the lake water level fluctuations.

This study demonstrates that the use of satellite-derived data such as water surface temperature can improve the water budget estimation in large lakes through considering spatial distribution of the key variables. Spatial distribution of parameters other than the water surface temperature (e.g., water quality and meteorological variables) may be also substantial in large lakes. Including such spatial variations through the use of validated satellite data in estimation of the water budget in large lakes can improve the accuracy of the water allocation decisions, and results in an enhanced water and ecosystem management.

Acknowledgments

The authors express their greatest gratitude and appreciation to Mr. Salmanian, Mr. Javidan and Mr. Bashirpur from the West Azerbaijan Regional Water Authority for providing in situ temperature data of Urmia Lake. We are also grateful to Mr. Luke Ginger for his review and assistance in improving the language of the paper.

References

Adams, W. P., & Prowse, T. D. (1981). Evolution and magnitude of spatial patterns in the winter cover of temperate lakes. *Fennia*, *159*(2), 343–359.
Ahmadzadeh Kokya, B., & Ahmadzadeh Kokya, T. (2008). Proposing a formula for evaporation measurement from salt water resources. *Hydrological Processes*, *22*, 2005–2012.
Alcântara, E. H., Stech, J. L., Lorenzzetti, J. A., Bonnet, M. P., Casamitjana, X., Assireu, A. T., et al. (2010). Remote sensing of water surface temperature and heat flux over a tropical hydroelectric reservoir. *Remote Sensing of Environment*, *114*, 2651–2665.
Benduhn, F., & Renard, P. (2004). A dynamic model of the Aral Sea water and salt balance. *Journal of Marine Systems*, *47*, 35–50.
Bowen, I. S. (1926). The ratio of heat losses by conduction and by evaporation from any water surface. *Physical Review*, *27*, 779–787.
Budyko, M. I. (1974). *Climate and life*. New York: Academic Press, 508.
Bussières, N., Verseghy, D., & MacPherson, J. I. (2002). The evolution of AVHRR-derived water temperatures over boreal lakes. *Remote Sensing of Environment*, *80*, 373–384.
Chavula, G., Brezonik, P., Thenkabail, P., Johnson, T., & Bauer, M. (2009). Estimating the surface temperature of Lake Malawi using AVHRR and MODIS satellite imagery. *Physics and Chemistry of the Earth*, *34*, 749–754.
Clark, N. E., Eber, L., Laurus, R. M., Renner, J. A., & Saur, J. F. T. (1974). *Heat exchange between ocean and atmosphere in the eastern North Pacific for 1961–71*. NOAA Technical Report NMFS (SSRF-682).
Coll, C., Caselles, V., Galve, J. M., Valor, E., Niclòs, R., Sánchez, J. M., et al. (2005). Ground measurements for the validation of land surface temperatures derived from AATSR and MODIS data. *Remote Sensing of Environment*, *97*, 288–300.
Crosman, E. T., & Horel, J. D. (2009). MODIS-derived surface temperature of the Great Salt Lake. *Remote Sensing of Environment*, *113*, 73–81.
Department of Environment (2010). *Integrated management plan for Lake Urmia Basin* (1st ed.) (prepared in Cooperation with UNEP/GEF).
Donlon, C. J., Minnett, P. J., Gentemann, C., Nightingale, T. J., Barton, I. J., Ward, B., et al. (2002). Toward improved validation of satellite sea surface skin temperature measurements for climate research. *Journal of Climate*, *15*, 353–369.
Gao, H., Birkett, C., & Lettenmaier, D. P. (2012). Global monitoring of large reservoir storage from satellite remote sensing. *Water Resources Research*, *48*, W09504.
Gianniou, S. K., & Antonopoulos, V. Z. (2007). Evaporation and energy budget in Lake Vegoritis, Greece. *Journal of Hydrology*, *345*(3), 212–223.
Gunaji, N. N. (1968). Evaporation investigations at Elephant Butte Reservoir in New Mexico. *International Association of Scientific Hydrology*, *78*, 308–325.
Harbeck, G. E. J., Kohler, M. A., & Koberg, G. E. (1958). *Water-loss investigations: Lake Mead studies*. Professional Paper, *298*, US Geological Survey.
Harris, A. R., & Mason, I. M. (1992). An extension of the split-window technique giving improved atmospheric correction and total water vapor. *International Journal of Remote Sensing*, *13*, 881–892.
Harrocks, L. A., Candy, B., Nightingale, T. J., Saunders, R. W., O'Carroll, A., & Harris, A. R. (2003). Parameterizations of the ocean skin-effect and implications for satellite-based measurement of sea surface temperature. *Geophysical Research*, *108*, 3096.

Hassanzadeh, E., Zarghami, M., & Hassanzadeh, Y. (2012). Determining the main factors in declining Urmia Lake level by using system dynamics modeling. *Water Resources Management*, *26*(1), 129–145.

Heidari, N., Roudgar, M., & Ebrahimpour, N. (2010). Thermodynamic quantities and Urmia Sea water evaporation. *Saline Systems*, *6*, 3.

Hook, S., Prata, F., Alley, R., Abtahi, A., Richards, R., Schladow, S., et al. (2003). Retrieval of lake bulk and skin temperature using along-track scanning radiometer (ATSR-2) data: A case study using Lake Tahoe, California. *Atmospheric and Oceanic Technology*, *20*, 534–548.

Hook, S. J., Vaughan, R. G., Tonooka, H., & Schladow, S. G. (2007). Absolute radiometric inflight validation of mid infrared and thermal infrared data from ASTER and MODIS on the Terra Spacecraft using the Lake Tahoe, CA/NV, USA, automated validation site. *IEEE Transactions on Geoscience and Remote Sensing*, *45*(6), 1798–1807.

Horne, A. J., & Glodman, C. R. (1994). *Limnology* (2nd ed.)New York: McGraw-Hill, Inc (575 pp.).

Jamab Consulting Engineering (1998). *Iran Integrated Water Management Project.* Urmia River Basin, Ministry of Energy (In Persian).

Jamali, M., & Marjani, A. A. (2007). Flow and salinity variation in a large hyper-saline lake in north of Iran. *AGU Fall Meeting 2007, San Francisco, CA, USA, 10–14 December 2007.*

Justice, C. O., Vermote, E., Townshed, J. R. G., Defries, R., Roy, D. P., Hall, D. K., et al. (1998). The moderate resolution imaging spectroradiometer (MODIS): Land remote sensing for global change research. *IEEE Transactions on Geoscience and Remote Sensing*, *36*, 1228–1247.

Karbassi, A., Bidhendi, G., Pejman, A., & Bidhendi, M. (2010). Environmental impacts of desalination on the ecology of Lake Urmia. *Journal of Great Lakes Research*, *36*(3), 419–424.

Keijman, Q. (1974). The estimation of the energy balance of a lake from simple weather data. *Boundary-Layer Meteorology*, *7*, 399–407.

Langer, M., Westermann, S., & Boike, J. (2010). Spatial and temporal variations of summer surface temperatures of wet polygonal tundra in Siberia — Implications for MODIS LST based permafrost monitoring. *Remote Sensing of Environment*, *114*, 2059–2069.

Lensky, N. G., Dvorkin, Y., & Lyakhovsky, V. (2005). Water, salt, and energy balances of the Dead Sea. *Water Resources Research*, *41*, 1–13.

Lenters, J. D., Kratz, T. K., & Bowser, C. J. (2005). Effects of climate variability on lake evaporation: Results from a long-term energy budget study of Sparkling Lake, northern Wisconsin (USA). *Journal of Hydrology*, *308*, 168–195.

Lerman, A., Imboden, D., & Gat, J. (1995). *Physics and chemistry of lakes*, *334*. (pp. 2) Berlin, Heidelberg, New York: Aufl. Springer-Verlag, 2.

Liu, W. L., Field, R. T., Gantt, R., & Klemas, V. (1987). Measurement of the surface emissivity of turbid waters. *Remote Sensing of Environment*, *21*, 97–109.

Lyons, R. P., Kroll, C. N., & Scholz, C. A. (2011). An energy-balance hydrologic model for the Lake Malawi Rift Basin, East Africa. *Global and Planetary Change*, *75*, 83–97.

Martin, S. (2005). *An introduction to ocean remote sensing.* New York: Cambridge University Press (426 pp.).

Masuda, K., Takashima, T., & Takayama, Y. (1988). Emissivity of pure seawaters for the model sea surface in the infrared window regions. *Remote Sensing of Environment*, *24*, 313–329.

McAtee, B., Pearce, A., Lynch, M., Davies, J., Boterhoven, M., & Osborne, B. (2007). The Hillarys Transect (2): Validation of satellite-derived sea surface temperature in the Indian Ocean off Perth, Western Australia. *Continental Shelf Research*, *27*(12), 1702–1718.

Meguro, H., Toba, Y., Murakami, H., & Kimura, N. (2004). Simultaneous remote sensing of chlorophyll, sea ice and sea surface temperature in the Antarctic waters with special reference to the primary production from ice algae. *Advances in Space Research*, *33*(7), 1168–1172.

Melesse, A. M., Abtew, W., & Dessalegne, T. (2009). Evaporation estimation of Rift Valley Lakes: Comparison of models. *Sensors*, *9*, 9603–9615.

Meyer, A. F. (1915). Computing run-off from rainfall and other physical data. *Transactions of the American Society of Civil Engineers*, *79*, 1056–1224.

Myrup, L., Powell, T., Godden, D., & Goldman, C. (1979). Climatological estimate of the average monthly energy and water budgets of Lake Tahoe, California–Nevada. *Water Resources Research*, *15*(6), 1499–1508.

Nehorai, R., Lensky, I. M., Lensky, N. G., & Shiff, S. (2009). Remote sensing of the Dead Sea surface temperature. *Journal of Geophysical Research*, *114*, c05021.

Neumann, J. (1958). Tentative energy and water balances for the Dead Sea. *Bulletin of the Research Council of Israel*, *76*, 137–163.

Niclòs, R., Valor, E., Caselles, V., Coll, C., & Sánchez, J. M. (2005). In situ angular measurements of thermal infrared sea surface emissivity — Validation of models. *Remote Sensing of Environment*, *94*, 83–93.

Novo, E. L. M. M., Barbosa, C. C. F., Freitas, R. M., Shimabukuro, Y. E., Melack, J. M., & Pereira-Filho, W. (2006). Seasonal changes in chlorophyll distribution in Amazon floodplain lakes derived from MODIS images. *Limnology*, *7*, 153–161.

Oesch, D. C., Jaquet, J., Hauser, A., & Wunderle, S. (2005). Lake surface water temperature retrieval using advanced very high resolution radiometer and moderate resolution imaging spectroradiometer data: Validation and feasibility study. *Journal of Geophysical Research*, *110*, C12014.

Oesch, D., Jaquet, J. -M., Klaus, R., & Schenker, P. (2008). Multi-scale thermal pattern monitoring of a large lake (Lake Geneva) using multi-sensor approach. *International Journal of Remote Sensing*, *29*(20), 5785–5808.

Ramsar Convention Website (na). http://ramsar.wetlands.org/Database

Reinart, A., & Reinhold, M. (2008). Mapping surface temperature in large lakes with MODIS data. *Remote Sensing of Environment*, *112*, 603–611.

Robinson, I. S., Wells, N. C., & Charnock, H. (1984). The sea surface boundary layer and its relevance to the measurement of sea surface temperature by airborne and space borne radiometers. *International Journal of Remote Sensing*, *5*, 19–45.

Rosenberry, D. O., Winter, T. C., Buso, D. C., & Likens, G. E. (2007). Comparison of 15 evaporation models applied to a small mountain lake in the northeastern USA. *Journal of Hydrology*, *340*(3–4), 149–166.

Rubin, H., & Atkinson, J. (2001). *Environmental fluid mechanics.* New York: Marcel Dekker (728 pp.).

Sadra Counsulting Engineers (2005). *Design & construction of the Oromieh lake causeway: Hydrodynamic & hydraulic and environmental (sediment & salinity) investigation report ministry of roads & transportation.*

Salhotra, A. M., Adams, E. E., & Harleman, D. R. F. (1985). Effect of salinity and ionic composition on evaporation: Analysis of the Dead Sea evaporation pans. *Water Resources Research*, *21*, 1336–1344.

Savtchenko, A., Ouzounov, D., Ahmad, S., Acker, J., Leptoukh, G., Koziana, J., et al. (2004). Terra and Aqua MODIS products available from NASA GES DAAC. *Advances in Space Research*, *34*(4), 710–714.

Schneider, P., & Hook, S. J. (2010). Space observations of inland water bodies show rapid surface warming since 1985. *Geophysical Research Letters*, *37*, L22405.

Schneider, P., Hook, S. J., Radocinski, R. G., Corlett, G. K., Hulley, G. C., Schladow, S. G., et al. (2009). Satellite observations indicate rapid warming trend for lakes in California and Nevada. *Geophysical Research Letters*, *36*, L22402.

Sima, S., Ahmadalipour, A., Shafiee Jood, M., & Tajrishy, M. (2012). Monitoring Urmia Lake area variation using MODIS Satellite data. *World Environmental and Water Resources Congress 2012* (Albuquerque, New Mexico, United States May 20–24, 1917–1926).

Small, E. E., Sloan, L. C., Hostetler, S., & Giorgi, F. (1999). Simulating the water balance of the Aral Sea with a coupled regional climate-lake model. *Journal of Geophysical Research*, *104*(D6), 6583–6602.

Steissberg, T. E., Hook, S. J., & Schladow, S. G. (2005). Characterizing partial upwellings and surface circulation at Lake Tahoe, California–Nevada, USA with thermal infrared images. *Remote Sensing of Environment*, *99*, 2–15.

Sturrock, A. M., Winter, T. C., & Rosenberry, D. O. (1992). Energy budget evaporation from Williams Lake: A closed lake in north central Minnesota. *Water Resources Research*, *28*(6), 1605–1617.

Sumner, M. D., Michael, K. J., Bradshaw, C. J. A., & Hindell, M. A. (2003). Remote sensing of Southern Ocean sea surface temperature: Implications for marine biophysical models. *Remote Sensing of Environment*, *84*(2), 161–173.

Thiemann, S., & Schiller, H. (2003). Determination of the bulk temperature from NOAA/AVHRR satellite data in a midlatitude lake. *International Journal of Applied Earth Observation and Geoinformation*, *4*, 339–349.

UNEP & GEAS (). The drying of Iran's Lake Urmia and its environmental consequences. *Journal of Environmental Development*, *2*, 128–137.

UNESCO (1983). *Algorithms for computation of fundamental properties of seawater.* UNESCO technical papers in marine science, *44*, (53 pp.).

Vallet-Coulomb, C., Legesse, D., Gasse, F., Travi, Y., & Chernet, T. (2001). Lake evaporation estimates in tropical Africa from limited meteorological data. *Journal of Hydrology*, *245*, 1–18.

Wan, Z. (1999). MODIS land-surface temperature algorithm theoretical basis document (LST ATBD). Version 3.3. http://modis.gsfc.nasa.gov/data/atbd/atbd_mod11.pdf

Wan, Z. (2006). *MODIS land surface temperature products user's guide.* Santa Barbara, CA: Institute for Computational Earth System Science, University of California.

Wan, Z. (2008). New refinements and validation of the MODIS land-surface temperature/emissivity products. *Remote Sensing of Environment*, *112*(1), 59–74.

Wells, M. G., & Sherman, B. (2001). Stratification produced by surface cooling in lakes with significant shallow regions. *Limnology and Oceanography*, *46*, 1747–1759.

Winter, T. C. (1981). Uncertainties in estimating the water balance of lakes. *Water Resources Bulletin*, *17*(1), 82–115.

Winter, T., Buso, D., Rosenberry, D., Likens, G., Sturrock, A., Jr., & Mau, D. (2003). Evaporation determined by the energy-budget method for Mirror Lake, New Hampshire. *Limnology and Oceanography*, *48*(3), 995–1009.

Wu, X., & Smith, W. L. (1997). Emissivity of rough sea surface for 8–13 μm: Modeling and verification. *Applied Optics*, *36*, 2609–2619.

Yekom Consulting Engineers (2002). *Management plan for the Lake Uromiyeh ecosystem.* Report 1 of the EC-IIP environmental management project for Lake Uromiyeh.

Yin, X., & Nicholson, S. E. (1998). The water balance of Lake Victoria. *Hydrological Sciences Journal*, *43*, 789–811.

Zeinoddini, M., Bakhtiari, A., & Ehteshami, M. (2013). Wave–flow coupling effects on spatiotemporal variations of flow and salinity in a large hypersaline marine system: Lake Urmia, Iran. *Limnology*, *14*, 77–95.

Zeinoddini, M., Tofighi, M. A., & Vafaee, F. (2009). Evaluation of a dike type causeway impacts on the flow and salinity regimes in the Urmia Lake. *Journal of Great Lakes Research*, *35*(1), 13–22.